Syntectonic sedimentation effects on the growth of fold-and-thrust belts

Charlotte Fillon[1,2], Ritske S. Huismans[2], and Peter van der Beek[1]
[1]Institut des Sciences de la Terre, Université Joseph Fourier, BP53, 38041 Grenoble, France
[2]Department of Earth Science, Bergen University, Bergen N-5007, Norway

ABSTRACT

We use two-dimensional mechanical models to investigate the effects of syntectonic sedimentation on fold-and-thrust belt development, testing variable syntectonic (wedge-top and foredeep) sediment thicknesses and flexural rigidities. Model results indicate a first-order control of syntectonic sedimentation on thrust-sheet length and thrust spacing. Thrust sheets are longer when syntectonic sediment thickness and/or flexural rigidity increase. Comparison with observations from several fold-and-thrust belts confirms this first-order control of syntectonic sedimentation.

INTRODUCTION

The potential controls of surface processes on the tectonic evolution of mountain belts are slowly becoming better understood (e.g., Whipple, 2009). Whereas erosion can strongly influence the growth of orogenic hinterland regions (Beaumont et al., 1992; Willett, 1999), syntectonic sedimentation appears as a dominant control on external fold-and-thrust belt development (Bonnet et al., 2007; Boyer, 1995; Huiqi et al., 1992; Malavieille, 2010; Marshak and Wilkerson, 1992; Mugnier et al., 1997; Simpson, 2006; Stockmal et al., 2007; Storti and McClay, 1995). Erosion products from the core of a mountain belt are transported to the foreland and deposited while the orogenic wedge continues to grow, thus interacting with the development of the fold-and-thrust belt.

This interaction can be understood in terms of critical taper theory (Dahlen, 1984, 1990; Davis et al., 1983): sedimentation on top of the wedge increases the taper angle necessary to reactivate and create new internal thrusts, thus promoting wedge propagation on the décollement level; sedimentation on the lower part of the wedge has the opposite effect.

The influence of erosion and sedimentation on the structural development of fold-and-thrust belts has been studied principally using analogue models. Storti and McClay (1995), for example, showed that adding syntectonic sediments on top of a wedge reduces the number of thrusts, the internal shortening, and the taper angle required for the wedge to be critical, leading to longer thrust sheets. The surface slope and geometry of fold-and-thrust belts are also affected by flexural controls on plate bending, which are not easily incorporated in analogue models (but see Hoth et al., 2007). Numerical models of fold-and-thrust belt development integrate these effects more easily, and have now reached sufficiently high numerical resolution that their predictions can be compared with observations in natural systems (Stockmal et al., 2007). Here we use two-dimensional (2-D) mechanical models to investigate depositional controls on fold-and-thrust belt development.

Focusing in particular on the effects of syntectonic wedge-top and foredeep sedimentation and the influence of flexure, we show that both exert first-order controls on wedge geometry and thrust propagation: increasing the thickness of syntectonic sediments and/or flexural rigidity leads to the activation of fewer and longer thrust sheets. We show that these general results are consistent with observational constraints on structure and syntectonic sedimentation in natural fold-and-thrust belts.

MODEL SET UP

We use a 2-D arbitrary Lagrangian-Eulerian (ALE) finite-element technique (Fullsack, 1995) to model thin-skinned fold-and-thrust belt development. The model consists of strain-weakening frictional-plastic materials that allow for localization of deformation (Stockmal et al., 2007; Huismans and Beaumont, 2003; see the GSA Data Repository[1] for details).

The reference model (Fig. 1) consists of four materials: (I) a strong strain-weakening frictional-plastic material, representing basement rocks; (II) an intermediate-strength strain-weakening frictional-plastic material representing sedimentary rocks; (III) a very weak frictional-plastic internal décollement layer between these two, representing evaporites; and (IV) a second weak frictional-plastic décollement layer located at the base of the model. The initial geometry resembles a pre-existing wedge and an adjacent sedimentary basin. A 1 cm yr^{-1} velocity boundary condition is imposed on the right side and the base of the model (Fig. 1). The left side of the model domain is fixed horizontally, except at the base, where the basal décollement layer is evacuated at the same velocity. Gravitational loading is compensated by flexural isostasy.

Here we focus exclusively on the effects of sedimentation and do not include erosional processes. Syntectonic sedimentation starts at 5 m.y. in models 2–6. From that moment, all topography below a fixed reference height, representing base level, is filled with sediments (Fig. 1). This representation of sedimentation is very simple but is consistent with the first-order infilling geometry of an orogenic wedge and its foreland basin system (e.g., DeCelles and Giles, 1996): the accommodation space is filled by sediments that are subsequently deformed, and the elevation of the reference level forces sedimentation to occur only in the foredeep and wedge-top domains. Varying base level allows for testing the effect of varying sediment input to the foreland.

MODEL RESULTS

We present two sets of models that demonstrate the sensitivity to syntectonic sedimentation (Fig. 2) and to flexural rigidity (Fig. 3). The first set includes three models with no (model 1), moderate (model 2), and strong (model 3) syntectonic sedimentation. The second set investigates the response to changes in flexural rigidity (from 10^{21} to 10^{23} N m) for moderate sedimentation.

Reference Model, No Deposition—Model 1

During the first 5 m.y., deformation only affects the strong basement, building an initial high-relief orogenic wedge with a system of pro-thrusts and retro-thrusts (Fig. 2A), a
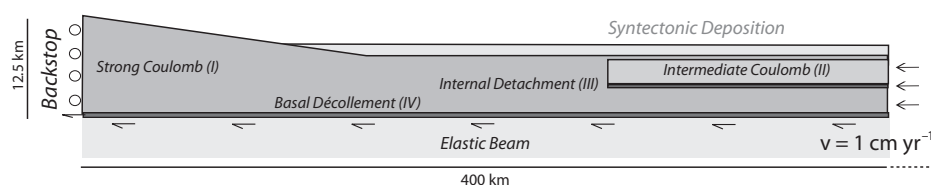
Figure 1. Model geometry and boundary conditions (v is velocity). Dotted line on right side of box represents continuity of the Lagrangian grid up to 800 km from the backstop; Eulerian grid extends to 400 km. Syntectonic deposition starts at 5 m.y. See text and Table DR1 (see footnote 1) for model parameter values.
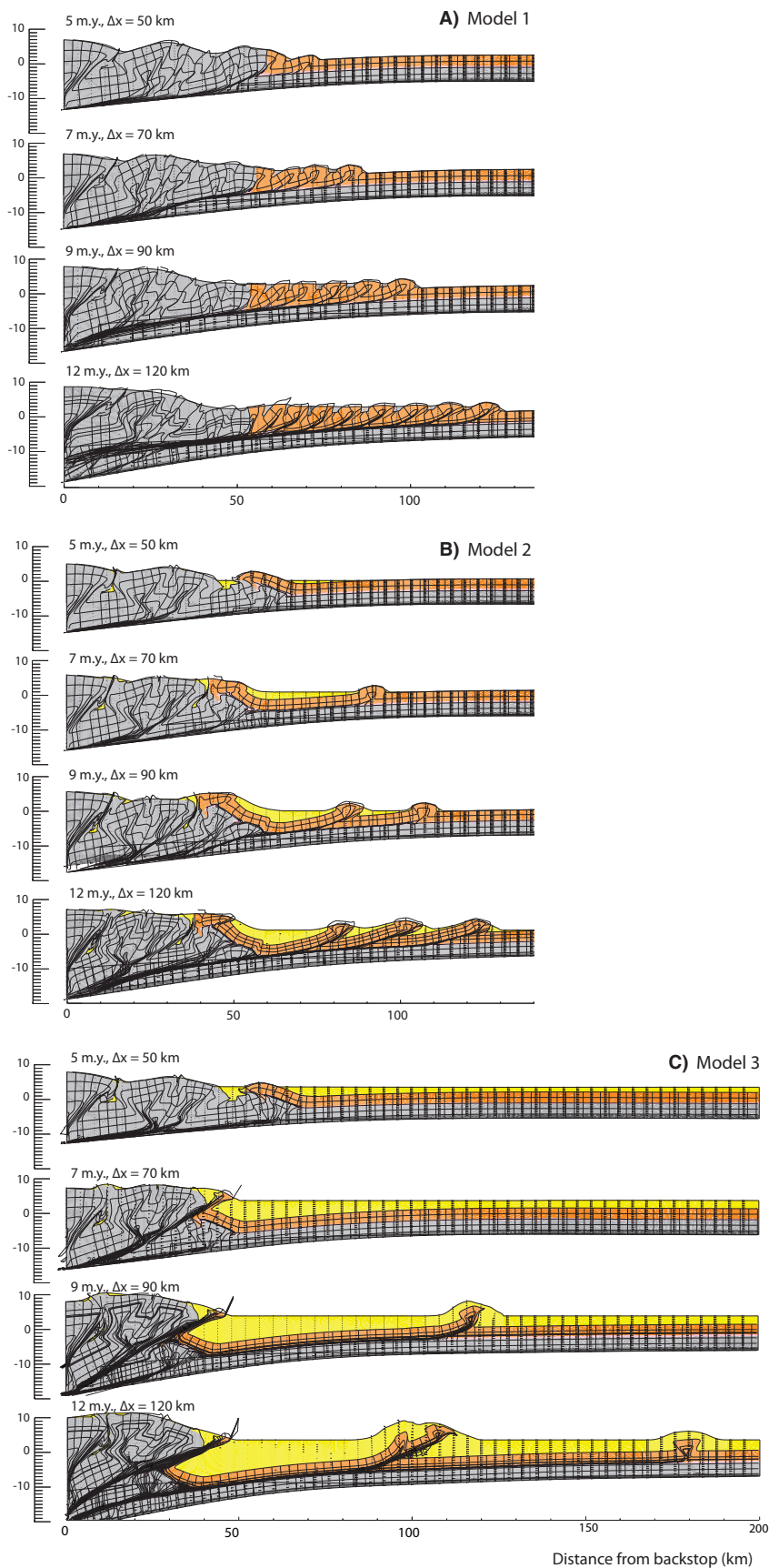
Figure 2. Model evolution with different amounts of syntectonic sedimentation. A: Model 1, no syntectonic sedimentation. B: Model 2, syntectonic sedimentation up to 1.95 km elevation. C: Model 3, syntectonic sedimentation up to 3 km elevation. Panels show development at 5, 7, 9, and 12 m.y. Flexural rigidity is 10^{22} Nm.

common feature of all the models presented. After 5 m.y., deformation propagates to the intermediate-strength pre-tectonic sedimentary rocks that deform contemporaneously with the hinterland wedge. From this time on, short thrusts develop in sequence. All thrusts verge toward the foreland with a regular spacing of ~17 km. No backthrusts develop, and there is almost no reactivation or out-of-sequence thrusting. By 12 m.y., nine uniform-length thrust sheets have formed.

Moderate Deposition—Model 2

Model 2 includes syntectonic sedimentation up to an intermediate reference level after 5 m.y. (Fig. 2B). At 5 m.y., the pre-tectonic sedimentary rocks are back-thrusted while a basement duplex develops in the hinterland; syntectonic sedimentation occurs mainly in the foredeep area. The first frontal thrust initiates at 7 m.y., creating a 34-km-wide wedge-top basin. With further shortening, deformation migrates back into the internal parts of the wedge and is partitioned between frontal and basal accretion. At 9 m.y., flexural subsidence resulting from the growing internal wedge, provides more sediment accommodation space and the formation of a second smaller wedge-top basin between the two frontal thrusts. At 12 m.y., deformation is partitioned between the frontal thrust, the reactivated back-thrust, and internal basement deformation. The average thrust-sheet length is 30 km, and the maximum sediment thickness is 4 km.

Strong Deposition—Model 3

The generic behavior of model 3 is similar to model 2, but the increased sediment thickness results in longer thrust sheets (Fig. 2C). The first external thrust emerges at ~9 m.y., at ~100 km from the backstop, resulting in a 75-km-wide wedge-top basin. The frontal thrust breaks through the sediments, where they start forming a constant thickness foreland basin fill. At 9 m.y., shortening is still accommodated by the frontal thrust, which accumulates more displacement than in model 2. A second thrust initiates just before 12 m.y. The average thrust-sheet length is 70 km with a maximum sediment thickness of 9 km.

Sensitivity to Flexural Rigidity—Models 4–6

Models 4–6 test the sensitivity to variations in flexural rigidity for a constant intermediate base level, and are all shown at 8 m.y. (Fig. 3). Model 5, which has the reference model rigidity (10^{22} Nm), is very similar to model 2. A lower flexural rigidity (model 4; 10^{21} Nm) favors a narrow foreland basin and the formation of a shorter (34-km-long) thrust sheet. In contrast, a higher flexural rigidity (model 6; 10^{23} Nm) favors the development of a wide foreland basin and the formation of a 94-km-long thrust sheet.
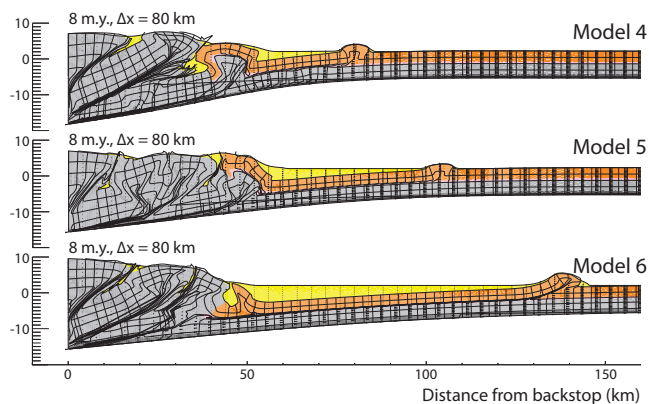
Figure 3. Sensitivity to flexural rigidity. Panels show evolution at 8 m.y. for models 4–6 with varying flexural rigidity (model 4: 10^{21} Nm; model 5: 10^{22} Nm; model 6: 10^{23} Nm), corresponding to elastic thicknesses of 4.8, 10.4, and 22.4 km, respectively (for Poisson ratio of 0.25 and Young's modulus of 10^{11} Nm^{-2}). Models were run with syntectonic sedimentation reference level of 2.15 km.

DISCUSSION

The first-order evolution of all models is similar, independent of the amount of syntectonic sediments (Fig. 2): (1) initiation of a frontal thrust, (2) out-of-sequence internal deformation and passive retreat of the external thrust belt, and (3) initiation of a new in-sequence thrust, reproducing a frontal accretion cycle (e.g., Hoth et al., 2007; DeCelles and Mitra, 1995). The main differences between the models are the locus and the timing of thrust activation.

The model without synorogenic sedimentation propagates most rapidly. Thrusts are very short, numerous, and do not accommodate much shortening, whereas the thrust-sheet length increases with the amount and extent of syntectonic sedimentation.

The first external thrust and the subsequent frontal thrusts emerge either at the point where the sediments taper out (model 2) or where they start forming a constant-thickness foreland-basin fill (model 3). The location of thrust initiation corresponds to the point where the total work needed to slide on the décollement and to break through the sediments is minimal (Hardy et al., 1998). When sediment deposits extend further (model 3), the location of frontal thrust activation migrates toward the foreland. The extent and thickness of syntectonic sediments thus assert a first-order control on the location of the frontal thrusts.

The models presented here demonstrate that the extent and thickness of syntectonic sediments strongly affect the structural style of fold-and-thrust belts. The sediments are deposited horizontally, effectively stabilizing the wedge (e.g., Willett and Schlunegger, 2010). In the most external parts, where the sediments are thinnest and the angle of the basal décollement (β) tends to zero, the wedge reaches a critical state. After the formation of the first thrust the surface slope α strongly decreases, stabilizing the wedge. Further syntectonic sedimentation in front of the active thrust enlarges the stable wedge and promotes formation of a new frontal thrust. Therefore, the overall development of the wedge follows critical-taper theory. However the local-

ization and timing of thrust activation is strongly influenced by strain weakening and the evolution of the shear zones, which cannot be readily explained by the theory, as observed in other recent studies (Buiter, 2012; Simpson, 2011).

Flexure plays an important role in determining the structural style of a fold-and-thrust belt. The extent of sediment deposition is itself primarily governed by flexural parameters controlling the foreland basin shape. For lower flexural rigidities (Fig. 3, model 4) a narrow and deep

foreland basin is formed, limiting the extent of sedimentation with consequently shorter thrust sheets initiating where the sediments taper out. In contrast, for higher flexural rigidities, a wider foreland basin develops, promoting sedimentation much further out in the foreland and formation of longer thrust sheets.

The location of the frontal thrust is also affected by the strength of the décollement level. A stronger décollement renders frontal accretion more difficult (see the supplementary models in the Data Repository), but the reduction in thrust-sheet length is moderate (a few kilometers) compared to the effect of syntectonic sedimentation. Therefore, the role of décollement strength appears to be of secondary importance in controlling the geometry of fold-and-thrust belts.

COMPARISON TO NATURAL SYSTEMS

The numerical models presented here demonstrate that syntectonic sedimentation exerts a major control on fold-and-thrust belt development. We compare our results to observed structural style, syntectonic sediment thickness, and flexural rigidity of several thin-skinned fold-and-thrust belts around the world (Fig. 4). Cross
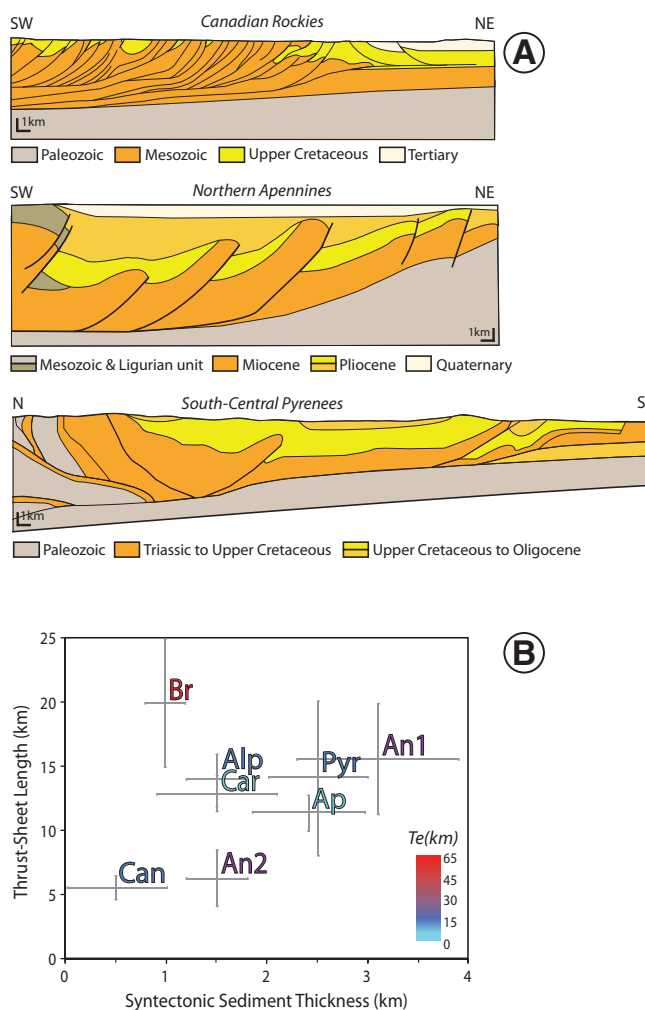
Figure 4. A: Simplified cross sections of fold-and-thrust belts with different thicknesses of syntectonic sediments and thrust-sheet lengths. From top to bottom: Canadian Rockies (Ollerenshaw, 1978), northern Apennines (Pieri, 1989), and ECORS (Etude Continentale et Oceanique par Reflexion et Refraction Sismique) section, Pyrenees (Muñoz, 1992). B: Average thrust-sheet length plotted against maximum sediment thickness (Te) for the Western Alps, France (Alp); sub-Andean belt, northwest Bolivia (An1) and south Bolivia (An2); northern Apennines (Ap); Brooks Range, Alaska (Br); Canadian Rockies (Can); Carpathians (Car) and southern Pyrenees (Pyr). The maximum sediment thickness and thrust-sheet length were measured on at least three thrust sheets of the fold-and-thrust belt and then averaged; see Table DR2 (see footnote 1) for values and references.

sections for three different fold-and-thrust belts (Pyrenees, Apennines, and Canadian Rockies) qualitatively illustrate the correlation between thrust-sheet length and syntectonic sediment thickness (Fig. 4A). The southern Pyrenean fold-and-thrust belt is characterized by a thick succession of syntectonic sediments, long thrust sheets, and a wide wedge-top basin, transported over an efficient décollement level, comparable to model 3 (Fig. 2C). The Apennines, with intermediate syntectonic sediment thickness, are characterized by moderate thrust-sheet length. The Canadian Rocky Mountains, where syntectonic sediments are thin or even absent, developed very short thrust sheets comparable to model 1 (Fig. 2A).

The average thrust-sheet length of eight fold-and-thrust belts is plotted as a function of maximum syntectonic sediment thickness in Figure 4B and according to the equivalent elastic thickness of the underlying lithosphere. Although these fold-and-thrust belts differ strongly in age and tectonic setting, a clear correlation appears between the thickness and extent of syntectonic sedimentation and thrust-sheet length. The effect of flexural rigidity is less obvious, although ranges developed on thicker elastic lithosphere appear to be characterized by the longest thrust sheets. Only the Brooks Range (Alaska) lies outside the observed trend. However, low-temperature thermochronology indicates that post-orogenic erosion has removed several kilometers of sediment from this range (O'Sullivan et al., 1997), so syntectonic deposits may have been much thicker initially. Including these sediments aligns this system with the observed trend.

CONCLUSIONS

We have presented mechanical models that provide a general explanation for the effects of syntectonic sedimentation on the formation of thin-skinned fold-and-thrust belts. The model results show that an increase in syntectonic sedimentation leads to significantly longer thrust sheets. Increases in flexural rigidity enhance this effect by widening the basin and therefore extending the area of sediment deposition. A range of natural thin-skinned fold-and-thrust belts shows a linear correlation between maximum sediment thickness and thrust-sheet length, confirming the inference from the numerical models.

REFERENCES CITED

Beaumont, C., Fullsack, P., and Hamilton, J., 1992, Erosional control of active compressional orogens, in McClay, K.R., ed., Thrust Tectonics: London, Chapman & Hall, p. 1–18.

Bonnet, C., Malavieille, J., and Mosar, J., 2007, Interactions between tectonics, erosion, and sedimentation during the recent evolution of the Alpine orogen: Analogue modeling insights: Tectonics, v. 26, TC6016, doi:10.1029/2006TC002048.

Boyer, S.E., 1995, Sedimentary basin taper as a factor controlling the geometry and advance of thrust belts: American Journal of Science, v. 295, p. 1220–1254, doi:10.2475/ajs.295.10.1220.

Buiter, S.J.H., 2012, A review of brittle compressional wedge models: Tectonophysics, v. 530–531, p. 1–17, doi:10.1016/j.tecto.2011.12.018.

Dahlen, F.A., 1984, Noncohesive Critical Coulomb wedges: An exact solution: Journal of Geophysical Research, v. 89, p. 10125–10133, doi:10.1029/JB089iB12p10125.

Dahlen, F.A., 1990, Critical taper model of fold-and-thrust belts and accretionary wedges: Annual Review of Earth and Planetary Sciences, v. 18, p. 55–99, doi:10.1146/annurev.ea.18.050190.000415.

Davis, D., Suppe, J., and Dahlen, F.A., 1983, Mechanics of fold-and-thrust belts and accretionary wedges: Journal of Geophysical Research, v. 88, p. 1153–1172, doi:10.1029/JB088iB02p01153.

DeCelles, P., and Giles, K.A., 1996, Foreland basin systems: Basin Research, v. 8, p. 105–123, doi:10.1046/j.1365-2117.1996.01491.x.

DeCelles, P.G., and Mitra, G., 1995, History of the Sevier orogenic wedge in terms of critical taper models, northeast Utah and southwest Wyoming: Geological Society of America Bulletin, v. 107, p. 454–462, doi:10.1130/0016-7606(1995)107<0454:HOTSOW>2.3.CO;2.

Fullsack, P., 1995, An arbitrary Lagrangian-Eulerian formulation for creeping flows and its application in tectonic models: Geophysical Journal International, v. 120, p. 1–23, doi:10.1111/j.1365-246X.1995.tb05908.x.

Hardy, S., Duncan, C., Masek, J., and Brown, D., 1998, Minimum work, fault activity and the growth of critical wedges in fold and thrust belts: Basin Research, v. 10, p. 365–373, doi:10.1046/j.1365-2117.1998.00073.x.

Hoth, S., Hoffmann-Rothe, A., and Kukowski, N., 2007, Frontal accretion: An internal clock for bivergent wedge deformation and surface uplift: Journal of Geophysical Research, v. 112, B06408, doi:10.1029/2006JB004357

Huiqi, L., McClay, K.R., and Powell, D., 1992, Physical models of thrust wedges, in McClay, K.R., ed., Thrust Tectonics: London, Chapman & Hall, p. 71–81.

Huismans, R.S., and Beaumont, C., 2003, Symmetric and asymmetric lithospheric extension: Relative effects of frictional-plastic and viscous strain softening: Journal of Geophysical Research, v. 108, p. 2496, doi:10.1029/2002JB002026.

Malavieille, J., 2010, Impact of erosion, sedimentation, and structural heritage on the structure and kinematics of orogenic wedges: Analog models and case studies: GSA Today, v. 20, p. 4–10, doi:10.1130/GSATG48A.1.

Marshak, S., and Wilkerson, M.S., 1992, Effect of overburden thickness on thrust belt geometry and development: Tectonics, v. 11, p. 560–566, doi:10.1029/92TC00175.

Mugnier, J.L., Baby, P., Colletta, B., Vinour, P., Bale, P., and Leturmy, P., 1997, Thrust geometry controlled by erosion and sedimentation: A view from analogue models: Geology, v. 25, p. 427–430, doi:10.1130/0091-7613(1997)025<0427:TGCBEA>2.3.CO;2.

Muñoz, J.A., 1992, Evolution of a continental collision belt: ECORS Pyrenees crustal balanced cross section, in McClay, K.R., ed., Thrust Tectonics: London, Chapman & Hall, p. 235–246.

O'Sullivan, P.B., Murphy, J.M., and Blythe, A.E., 1997, Late Mesozoic and Cenozoic thermotectonic evolution of the central Brooks Range and adjacent North Slope foreland basin, Alaska: Including fission track results from the Trans-Alaska Crustal Transect (TACT): Journal of Geophysical Research, v. 102, p. 20821–20845, doi:10.1029/96JB03411.

Ollerenshaw, N.C., 1978, Calgary, Alberta–British Columbia: Canada, Geological Survey of Canada, Map 1457A, scale 1:250000, 2 sheets.

Pieri, M., 1989, Three seismic profiles through the Po Plain, in Bally, A.W., ed., Atlas of Seismic Stratigraphy, Volume 27/3: Tulsa, Oklahoma, American Association of Petroleum Geologists, p. 90–110.

Simpson, G., 2011, Mechanics of non-critical fold-and-thrust belts based on finite element models: Tectonophysics, v. 499, p. 142–155, doi:10.1016/j.tecto.2011.01.004.

Simpson, G.D.H., 2006, Modelling interactions between fold-and-thrust belt deformation, foreland flexure and surface mass transport: Basin Research, v. 18, p. 125–143, doi:10.1111/j.1365-2117.2006.00287.x.

Stockmal, G.S., Beaumont, C., Nguyen, M., and Lee, B., 2007, Mechanics of thin-skinned fold-and-thrust belts: Insights from numerical models, in Sears, J.W., et al., eds., Whence the Mountains? Inquiries into the Evolution of Orogenic Systems: A Volume in Honor of Raymond A. Price, Geological Society of America Special Paper 433, p. 63–98, doi:10.1130/2007.2433(04).

Storti, F., and McClay, K., 1995, Influence of syntectonic sedimentation on thrust wedges in analogue models: Geology, v. 23, p. 999–1002, doi:10.1130/0091-7613(1995)023<0999:IOSSOT>2.3.CO;2.

Whipple, K.X., 2009, The influence of climate on the tectonic evolution of mountain belts: Nature Geoscience, v. 2, p. 97–104, doi:10.1038/ngeo413.

Willett, S.D., 1999, Orogeny and orography: The effects of erosion on the structure of mountain belts: Journal of Geophysical Research, v. 104, p. 28957–28981, doi:10.1029/1999JB900248.

Willett, S.D., and Schlunegger, F., 2010, The last phase of deposition in the Swiss Molasse Basin: From foredeep to negative-alpha basin: Basin Research, v. 22, p. 623–639, doi:10.1111/j.1365-2117.2009.00435.x.